# Supporting Information

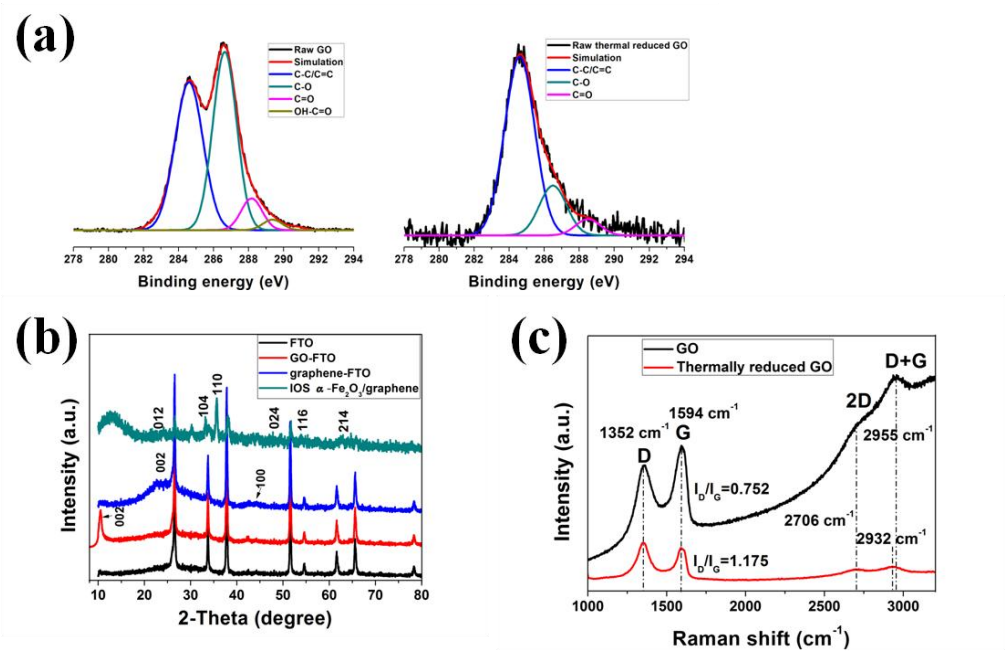


**Figure S1.** (a) C1s XPS spectra of GO and graphene film. (b) XRD patterns of GO, graphene and IOS α-$Fe_2O_3$/graphene film,

| Samples / Bonds | GO film | Graphene film |
|---|---|---|
| $A_{C-O}/A_{C-C/C=C}$ | 1.018 | 0.253 |
| $A_{C=O}/A_{C-C/C=C}$ | 0.161 | 0.076 |
| $A_{OH-C=O}/A_{C-C/C=C}$ | 0.019 | |

**Table S1.** The peak area (A) ratios of the oxygen-containing bonds to the C-C/C=C bonds for GO and graphene film.

The deconvoluted C1s peaks centered at the binding energies of 286.4, 286.6, 288.1, and 289.3 eV are assigned to the C-C/C=C, C-O, C=O and OH-C=O functional groups on the graphene oxide film surface, respectively [1]. After thermally reducing GO, the concentrations of these functional groups are remarkably decreased, the relative oxygen concentrations are calculated and summarized in Table S1.

The characteristic 2θ peak of GO film appearing at 11.07° corresponds to a d-spacing of approximately 7.984 Å. the substantial shift of the (002) reflection from 7.98 to 3.6 Å after reduction processing of GO confirms the formation of graphene from GO. These diffraction peaks can be readily indexed to rhombohedral α-$Fe_2O_3$. Almost similar peaks are observed in the XRD pattern of FTO prove this analysis.

The Raman spectrum of GO film displays two prominent peaks: ~1352 and ~1594 $cm^{-1}$, which corresponds to the well-documented D and G bands, respectively. The second order Raman feature, the 2D band at ~2706 $cm^{-1}$ and D+G bands at ~2955 $cm^{-1}$ is very sensitive to the stacking order of the graphene sheets along the c-axis as well as to the number of layers. G and D bands correspond to the in-plane vibration of $sp^2$ bonded carbon atoms [2] and the presence of $sp^3$ defects [3]. The intensity ratio for graphene film (1.175) shows an enhanced value compared to that for GO (0.752), indicating the presence of more localized sp3 defects within the sp2 carbon network after thermal reduction.

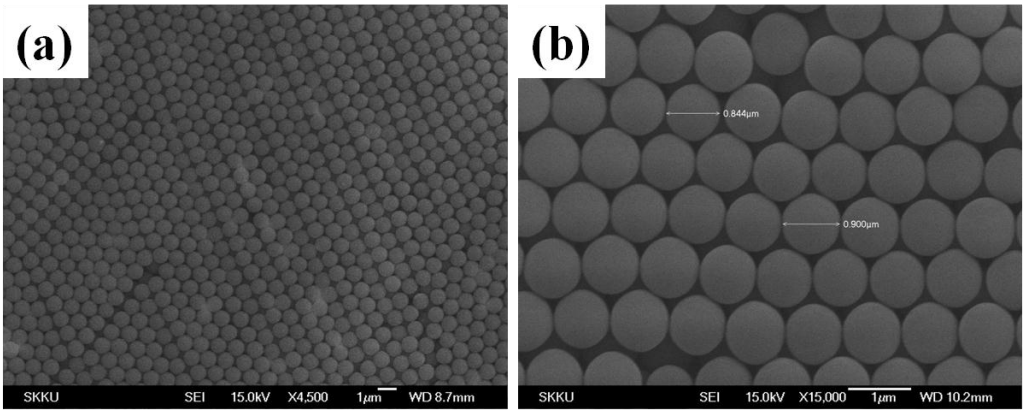


**Figure S2.** FE-SEM image of PS/graphene colloid templates.

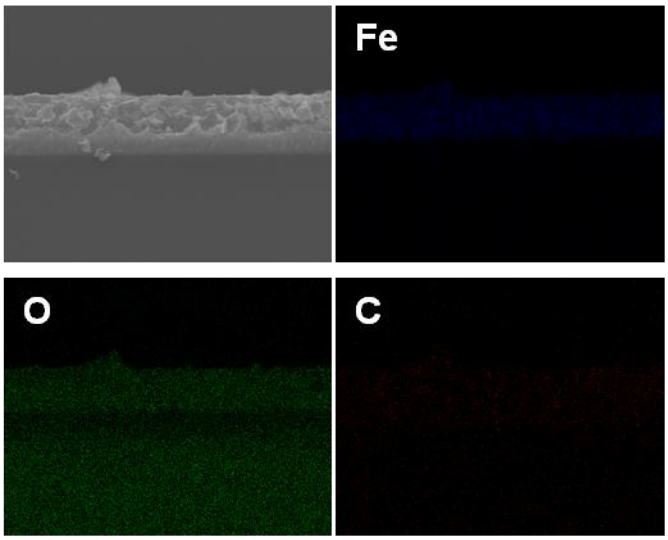


**Figure S3.** EDS elemental maps with Fe, O and C of α-$Fe_2O_3$/graphene/FTO film.

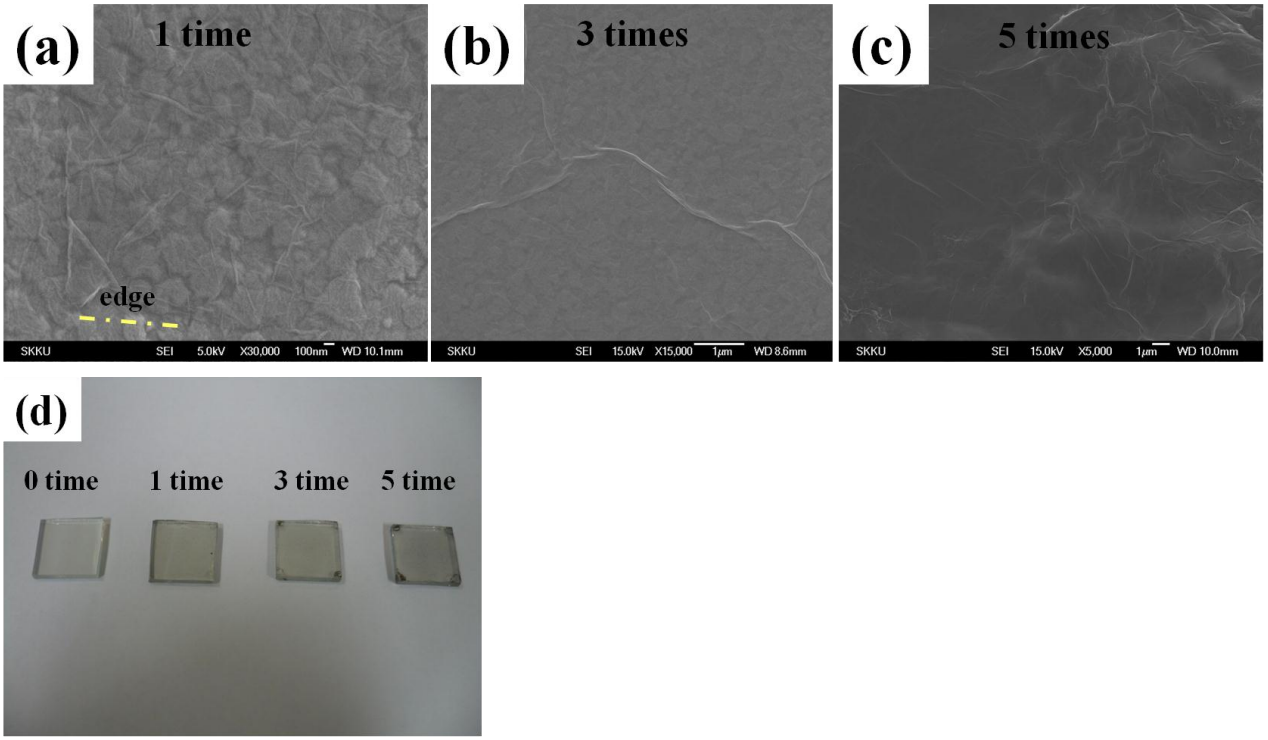


**Figure S4.** FE-SEM images (a-c) and photograph (d) of different layered graphene thin film.

FE-SEM images of different layered graphene film, from Fig. S5, it is clear to see that the FTO substrate gradually become unclear with increasing spin-coating time.

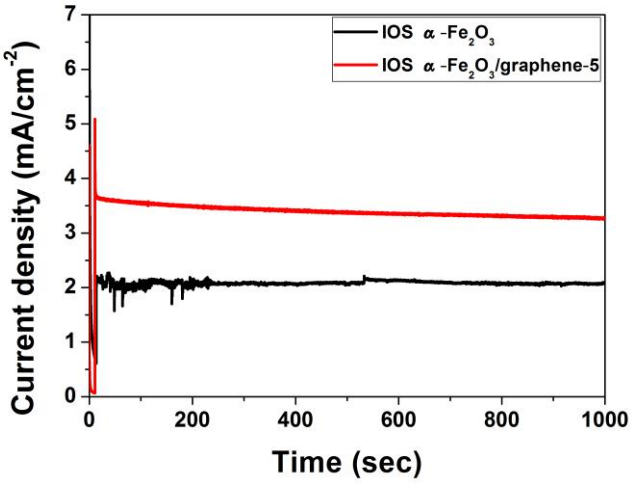


**Figure S5.** Long term of stability for α-$Fe_2O_3$ and α-$Fe_2O_3$/graphene-5 photoanodes under closed circuit conditions at applied potential of 0.5 V.

| Graphene coating time | Resistance (MΩ) |
|---|---|
| **1** | ∞ |
| **2** | ∞ |
| **3** | ∞ |
| **4** | ∞ |
| **5** | **~15** |
| **6** | **~2** |

**Table S2.** Resistance of graphene thin film on glass with different spin-coating times.

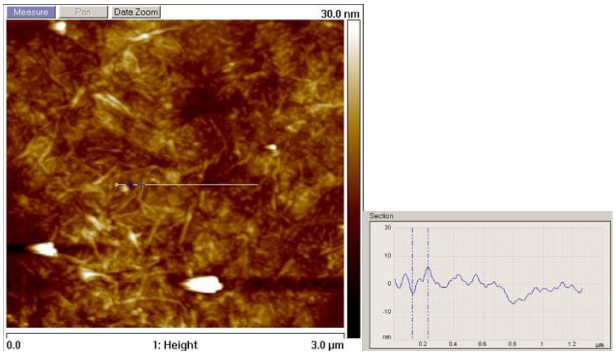


**Figure S6.** AFM image of graphene thin film with spin coating of 5 times.

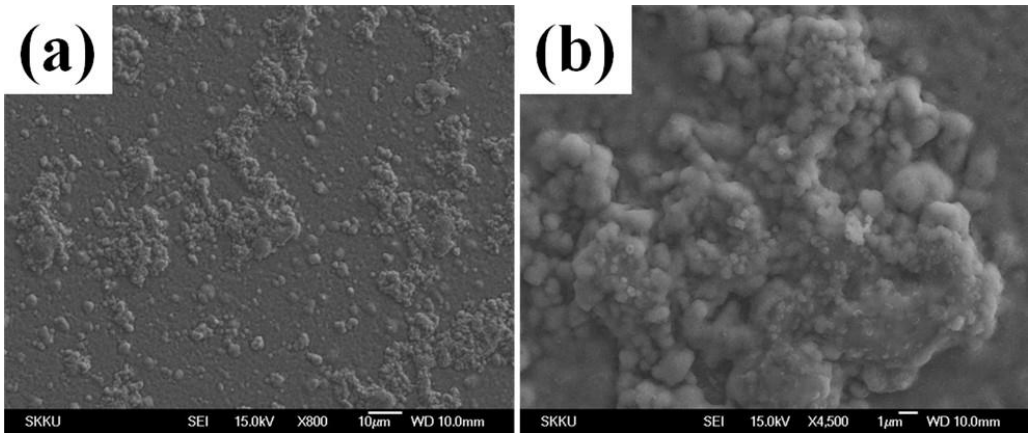


**Figure S7.** FE-SEM images of α-$Fe_2O_3$ film without any structure prepared by electrodeposition method.

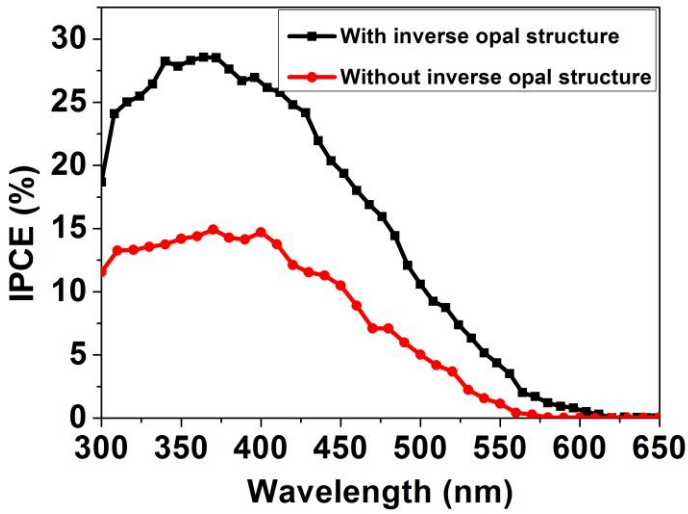


**Figure S8.** IPCE results of inverse opal structure and general structure α-$Fe_2O_3$ at 0.5 V vs Ag/AgCl under illumination by AM 1.5G light in 1 M NaOH electrolyte.

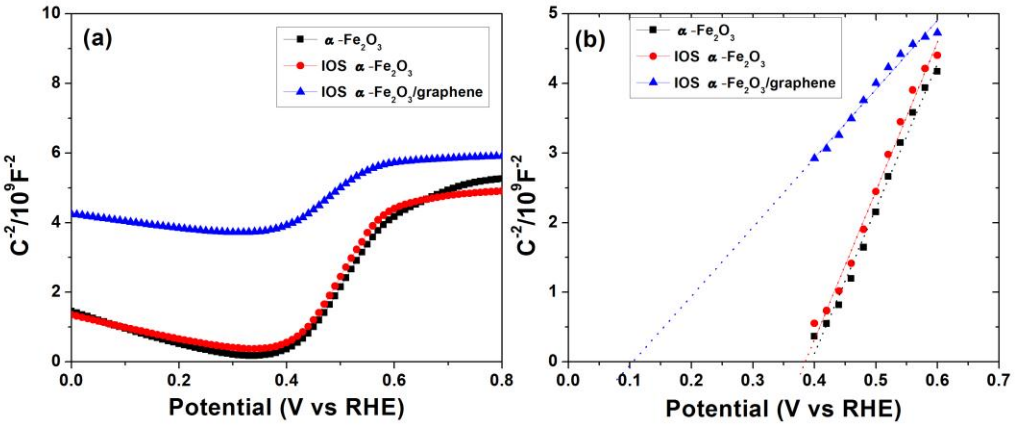


**Figure S9.** Mott-Schottky plots of α-$Fe_2O_3$, IOS α-$Fe_2O_3$ and IOS α-$Fe_2O_3$/graphene-5 electrodes in 0.5 M NaOH electrolyte.

Reversed sigmoidal plots were observed with an overall shape relevant to typical for n-type α-$Fe_2O_3$ (Figure S7a). The flat-band voltage (Vfb), which was calculated to be 0.41, 0.39 and 0.09 V vs RHE in 0.5 M NaOH electrolyte (equivalent to 0.61, 0.59 and 0.29 V vs. NHE) from the x intercepts of the linear region corresponding to α-$Fe_2O_3$, IOS α-$Fe_2O_3$ and IOS α-$Fe_2O_3$/graphene-5 (Figure S7b). It is well-known that Vfb equals the Fermi Level ($E_F$) for n-type semiconductors, and is an inherent property of such semiconductors[4]. In addition, the calculated $E_F$ of graphene is −0.08 eV vs NHE [5,6], which is more negative than the Fermi level of α-$Fe_2O_3$, resulting in hinder electron transfer from α-$Fe_2O_3$ to graphene. However, the accumulation of electrons inevitably causes shifting of the apparent Fermi level ($E_F$*) [7, 8], so that the Vfb of IOS α-$Fe_2O_3$/graphene-5 shifts negatively compared to that of IOS α-$Fe_2O_3$. On the other band, the $E_F$ of FTO is negative enough to accept electrons from α-$Fe_2O_3$ excited. Thus, the electronic interaction between graphene/FTO substrate and IOS α-$Fe_2O_3$ may cause a cathodic shift of the EF*, resulting in a higher conduction band position which allows charge transfer from α-$Fe_2O_3$ to graphene.

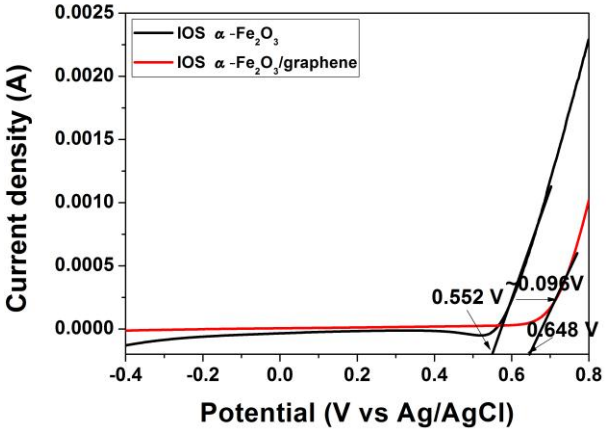


**Figure S10.** Dark current of IOS α-$Fe_2O_3$ and IOS α-$Fe_2O_3$/graphene-5 electrodes in 0.5 M NaOH electrolyte.

## Reference

[S1] Yang, D.; Velamakanni, A.; Bozoklu, G.; Park, S.; Stoller, M.; Piner, R.; Stankovich, S.; Jung, I.; Field, D., Jr.; Ruoff, R.; Chemical analysis of graphene oxide films after heat and chemical treatments by X-ray photoelectron and Micro-Raman spectroscopy. Carbon 2009, 47, 145–152

[S2] Zhang, W.; Cui, J.; Tao, C.; Wu, Y.; Li, Z.; Ma, L.; Wen, Y.; Li, G.; Strategy for Producing Pure Single-Layer Graphene Sheets Based on a Confined Self-Assembly Approach. Angewandte Chemie International Edition 2009, 48, 5864–5868.

[S3] Lu, J.; Yang, J.; Wang, J.; Lim, A.; Wang, S.; Loh, K.; One-Pot Synthesis of Fluorescent Carbon Nanoribbons, Nanoparticles, and Graphene by the Exfoliation of Graphite in Ionic Liquids. ACS Nano. 2009, 3, 2367–2375.

[S4] Scaife, D.; Oxide semiconductors in photoelectrochemical conversion of solar energy. Solar Energy 1980, 25, 41–54.

[S5] Wang, X.; Zhi, L.; Mullen, K.; Transparent, Conductive Graphene Electrodes for Dye-Sensitized Solar Cells. Nano Letters 2008, 8, 323–327

[S6] Khomyakov, P.; Giovannetti, G.; Rusu, P.; Brocks, G.; van den Brink, J.; Kelly, P.; First-principles study of the interaction and charge transfer between graphene and metals. Physical Reviewer B 2009, 79, 195425–195436.

[S7] Subramanian, V.; Wolf, E.; Kamat, P.; Catalysis with $TiO_2$/Gold Nanocomposites. Effect of Metal Particle Size on the Fermi Level Equilibration. Journal of the American Chemical Society 2004, 126, 4943–4950.

[S8] Kongkanand, A.; Kamat, P.; Electron Storage in Single Wall Carbon Nanotubes. Fermi Level Equilibration in Semiconductor–SWCNT Suspensions. ACS Nano 2007, 1, 13–21.